Paper AAS 97-726

Solar Electric Performance for Medlite and Delta Class Planetary Missions

Carl G. Sauer, Jr

Jet Propulsion Laboratory
California Institute of Technology
Pasadena, California 91109

AAS/AIAA Astrodynamics Specialist Conference

Sun Valley, Idaho. August 4-7, 1997

AAS Publications Office, P.O. Box 28130, San Diego, CA 92128

AAS 97-726

SOLAR ELECTRIC PERFORMANCE FOR MEDLITE AND DELTA CLASS PLANETARY MISSIONS"

Carl G. Sauer, Jr"

The current emphasis on small, low-cost planetary missions using Delta and Medlite Class launch vehicles has prompted the examination of the use of Solar Electric Propulsion (SEP) spacecraft to either enable or enhance the performance of some of the more demanding planetary missions. Planetary missions that appear most attractive for a small solar electric propulsion system include those missions that require a large post-launch AV commitment from the spacecraft propulsion system such as small body rendezvous and sample return missions. Other missions that may benefit from use of SEP would be a Mercury orbiter mission and various outer planet orbiter and flyby missions. The use of SEP for this latter class of missions could result in either increased performance or use of a smaller launch vehicle than that required for an equivalent chemically propelled ballistic mission.

INTRODUCTION

Preliminary estimates of planetary mission performance for small low-power SEP spacecraft were presented in two technical papers by the author[1,2] in 1993 and 1994. In these papers SEP trajectories were calculated based on a conceptually simple model of the propulsion system which assumed throttling of the thrusters under constant specific impulse and efficiency. Although the results presented in these papers demonstrated the feasibility of employing a small SEP powered spacecraft for planetary

---

* *The research described in this paper was performed by the Jet Propulsion Laboratory, California Institute of Technology, Pasadena, California under contract with the National Aeronautics and Space Administration*

"' *Senior Member of the Engineering* Staff, *Outer Planets Mission Analysis Croup, Navigation and Flight* Mechanics Section, *Senior Member* AAS, *Senior Member AIAA*

missions, better knowledge of the actual delivery capability using a more realistic model of thruster throttling is necessary for detailed mission and spacecraft design studies.

This first part of this paper describes the throttling behavior of the thrusters and the incorporation of this throttling behaviour into the SEP trajectory optimization formulation. A comprehensive set of SEP planetary missions based on this throttling behavior is presented in the second section of this paper. Two performance levels were examined in this mission study, a low power option using a single 30cm thruster and a Medlite (Delta 7326) launch vehicle, and a higher powered option using two 30 cm NSTAR thrusters and a Delta 7925. Since the Medlite has approximately one-half the injection capability of the Delta 7925 at low injection energies, a power level half that of the higher powered option was used which resulted in nearly identical interplanetary trajectories for these two performance levels.

THRUSTER THROTTLE CHARACTERISTICS

Extensive measurements of the throttling behavior of electric propulsion 2.5 kW 30 cm ion thrusters (NSTAR) have been made at the NASA Lewis Research Center in Cleveland[3] and at the Jet Propulsion Laboratory in Pasadena to support a technology verification of Solar Electric Propulsion. This verification of thruster technology will be flown on the New Millennium Deep Space 1 mission (DS1) which is currently scheduled to be launched in July 1998 and flyby the Asteroid 3352 McAuliffe and short period comet West-Koutek-Ikemura . In order to provide accurate and reliable estimates of mission performance, SEP throttle characteristics based upon the above measurements have been incorporated into the trajectory optimization software currently being used for Solar Electric Propulsion mission studies.

The modeling of the throttling consists of approximating both thrust and mass flow rate as polynomial functions of power processor input power. An example of polynomial fits to actual measurements of thruster throttling is shown in Figures 1 and 2.

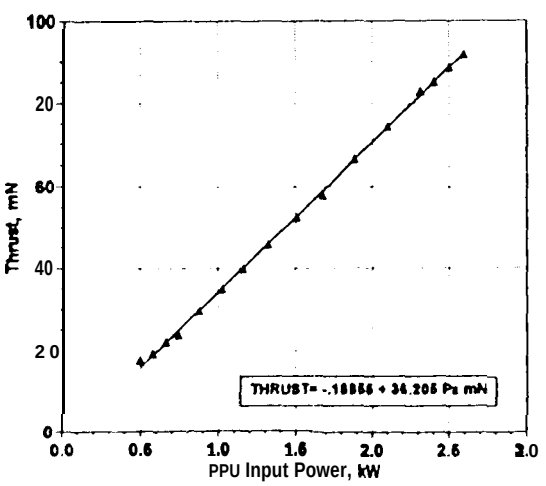

Figure 1 Thrust Level

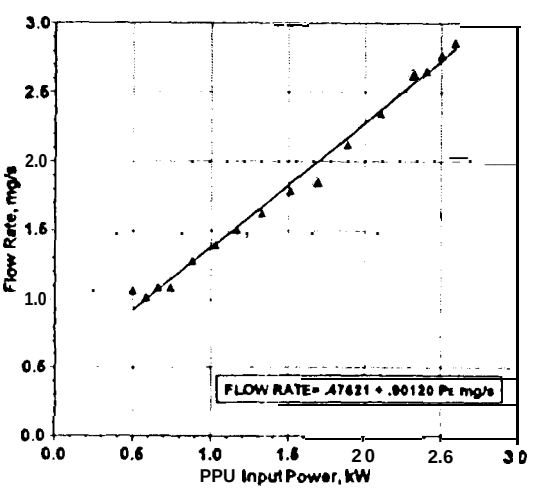

Figure 2 Mass Flow Rate

In these figures a linear fit of thrust force and mass flow rate to power processor input power was sufficient to approximate the throttle behavior since higher order polynomial fits did not result in significantly lower errors so as to justify their use. More recent measurement of thruster throttling indicate that higher order polynomial approximations are better justified however. It should be noted that the approximately 5 to 1 range of power processor input power dictate some rather severe requirements on thruster throttling. These thrusters were originally developed for use in high *power* propulsion systems with a power level sufficient to operate from 6 to 8 thrusters at a time. In this configuration it was possible to operate the propulsion system with various numbers of operating thrusters and it was only necessary to throttle the engines over about a 2 to 1 range. In order for these same thrusters to be used for the small low powered spacecraft where only one or two thrusters may be operating, it is necessary to throttle them over a much larger range in order to provide sufficient thrust for many of the planetary missions under consideration.

In order that both specific impulse and efficiency be constant, it is necessary that thrust and mass flow rate be linear functions of input power and both pass through the origin. Although both thrust and mass flow rate were fit as linear functions of thruster input power, an observation of these in Figures 1 and 2 indicate that neither, but in particular mass flow rate, pass through the origin. As a consequence both specific impulse and efficiency vary over the throttle range. The specific impulse and overall thruster efficiency which result from the fits to thrust and mass flow rate are shown in Figures 3 and 4 respectively and indicate the degree that the thruster performance degrades at the lower throttle levels. Since some of the planetary missions require thrusting at several astronomical units from the sun where thrusting is at the lower end of the throttle profile, it is important to model thruster performance to an accuracy sufficient to get reliable estimates of delivery capability. Note that both specific impulse and efficiency at the lowest throttle level drop to about half their values at maximum power.

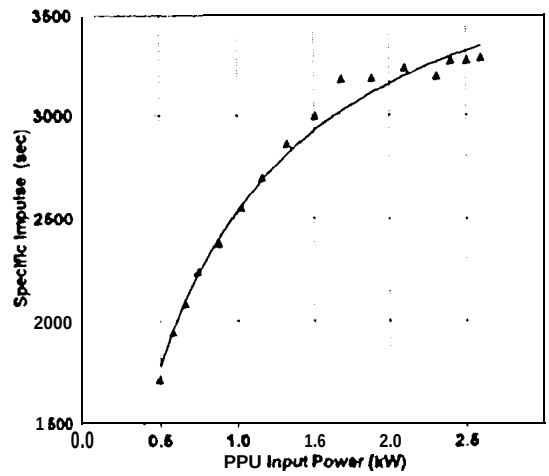

Figure 3 Specific Impulse

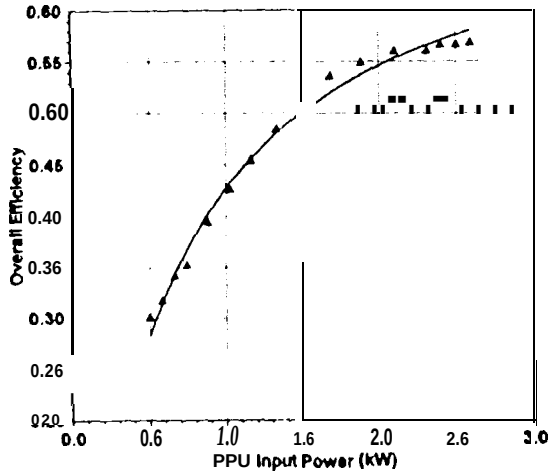

Figure *4* Thrust Efficiency

TRAJECTORY OPTIMIZATION

The kinematic aspects of the trajectory optimization *are* only briefly summarized here since they have been adequately treated elsewhere. In essence the SEP trajectory optimization consists of a simultaneous integration of the equations of motion and costate or variational equations. Terminal constraints and targeting are satisfied by subsequently solving a two point value problem. The Hamiltonian H for this formulation is given by,

$$H = -\left(p \cdot V + \dot{p} \cdot \nabla U \right) + H_A \tag{1}$$

where p is the costate vector conjugate to velocity and is otherwise identified as the Primer Vector. In the above equation V is the velocity vector and U is the gravitational potential and the term H_A is that part of the Hamiltonian that is a function of the propulsion and vehicle parameters This term is composed of two parts and is given by,

$$H_A = \frac{f}{m} p \cdot \zeta - \dot{m} p_m = \frac{f}{m} \left(p \cdot \zeta - \frac{m p_m}{c} \right) \tag{2}$$

where f is the magnitude of the thrust, c the exhaust velocity, m is the mass of the spacecraft, and ζ is the unit thrust vector. The variable p_m is the costate conjugate to spacecraft mass. The term enclosed in the brackets in Equation 2 is commonly referred to as the thrust switching function and is used to determine thrust and coast phases along the trajectory. Since this trajectory optimization has been formulated to maximize net spacecraft mass, the hamiltonian in the above equations can always be maximized by turning the thrust off whenever the term in the bracket in Equation 2 becomes negative. Note that the hamiltonian in Equation 2 is also maximized when the thrust vector and primer vector are co-linear.

The differential equations serving to define the position R and velocity V of the spacecraft are given by,

$$\dot{R} = V \tag{3}$$

and

$$\dot{V} = -\nabla U + \frac{f}{m} \zeta \tag{4}$$

The primer vector p is determined by integrating the second order differential equation

$$\ddot{p} = -\left(p \cdot \nabla \right) \nabla U - \frac{\partial H_A}{\partial R} \tag{5}$$

and the costate vector conjugate to spacecraft mass is found by integrating the first

order differential equation,

$$P_m = -\frac{\partial H_A}{\partial m} \tag{6}$$

To complete the definitions, the thrust and mass flow rate are given as functions of power processor input power by

$$f = N_T \sum_{i=0}^{n} a_i P_E^i \tag{7}$$

and

$$\dot{m} = N_T \sum_{i=0}^{n} b_i P_E^i \tag{8}$$

where N_T is the number of operating thrusters and the coefficients a and b in the above equations are those determined from the curve fit of thrust and mass flow rate. For the missions presented in this paper both thrust and mass flow rate are approximated as linear functions of input power so that n=l in both Equations 7 and 8.

The power available to an individual thruster is found by calculating the array output power, subtracting any fixed spacecraft or housekeeping power, and then dividing the remaining power by the number of operating thrusters. In the examples to be presented in this paper, only one mission, that of a comet sample return, allows thruster staging where different number of operating thrusters are allowed during the mission. All the other missions have a freed number of operating thrusters. In the comet sample return mission, the point where the thrusters are staged is calculated by examining the hamiltonian, HA, in Equation 2 for each allowable thruster state and selecting that thruster state which maximizes the value of H_A. H_A is also indirectly a function of the solar distance since the solar array output power varies as a function of distance from the sun. As a consequence the partial derivative with respect to position of HA must appear in the differential equation for the Primer Vector in Equation 5.

The model of the solar array* output power used in these trajectory simulations varies inversely with the square of heliocentric distance modified by a conversion efficiency that is a function of solar distance. The conversion efficiency for this array model is approximately 20 percent higher at 2 astronomical units than at the Earth and drops to below 80 percent at the distance of Venus. At a point slightly inside the orbit of Venus the array efficiency has decreased sufficiently so that the solar array must be tilted with respect to the sun direction in order to keep the array temperature and output power constant.

---

* *The* solar array *used for all* the missions except *the* Mercury *orbi ter is based on* Silicon *solar* cells, the *use of Gallium/Arsenide solar cel* 1s will *resul tin different performance because of their reduced* variation of *efficiency with temperature.*

Figure 5 shows the relative variation of solar array efficiency as a function of solar distance for both a typical Silicon array and a Gallium/Arsenide array. In the optimization program the actual power available from an array is found by taking the reference array power at the distance of the Earth, multiplying it by the relative array efficiency, and then dividing that power by the square of the solar distance. Values of relative array efficiency at solar distances beyond 2.5 to 3 astronomical units are considerably uncertain. However the only mission reported in this paper that actually requires thrusting at such large solar distances is that of the comet sample return mission; this being the reason that thruster staging is used because of the large variation of array output power.

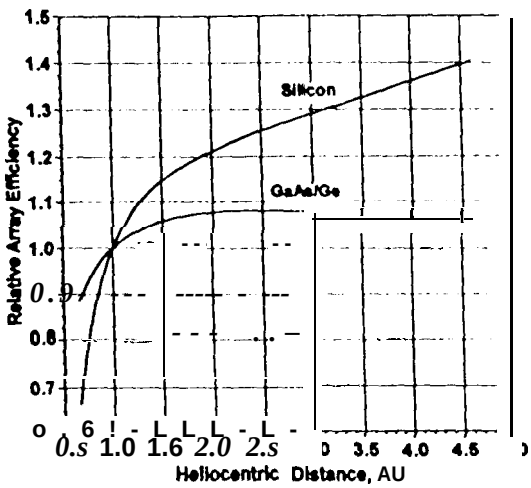

Figure 5 Relative Array Efficiency

LAUNCH VEHICLE AND PROPULSION SYSTEM DEFINITIONS

The performance for the two launch vehicles used in this paper is based on that given in the NASA Announcement of Opportunity for Discovery Missions issued in 1996. An allowance for launch vehicle to spacecraft adapter is included in this performance. In addition a 10% launch vehicle contingency is taken to account for various project reserves, non due east launches and other mission peculiarities.

Different thruster combinations are used in generating these SEP trajectories depending upon the launch vehicle and array power used. Since the maximum thruster power is 2.5 kW, only a single operating thruster is used for missions launched on a Medlite and only two operating thrusters are used for missions launched on the more capable Delta 7925. Although additional thrusters with larger solar arrays could be used, the increase in performance would be more than offset by the increase in propulsion system mass.

The nominal or reference solar array power is not necessarily that required to just operate one or two thrusters. For many missions such as asteroid or comet rendezvous missions, the variation of solar array output power can exceed the throttling range of 5 to 1 and the solar array power must be increased sufficiently so that power is

available at the maximum required thrusting distance. For the most of these planetary missions the reference array power was fixed at 3.375 kW for Medlite class missions with one operating thruster and twice that at 6.75 kW for the Delta class missions with two operating thrusters, Several missions, for instance the Ceres rendezvous mission and the comet sample return mission, require even larger array powers because of the greater solar distances where thrusting is required. However the Mercury orbiter mission is able to use a lower array power because this mission never goes beyond the orbit of the Earth. An allowance for a fixed spacecraft housekeeping power is also included, 125 watts is used for the Medlite class missions and 250 watts is used for the Delta class missions.

The total delivered spacecraft and propulsion system mass is used as an indication of performance for these missions. This indication of performance is used rather than net spacecraft mass because of the wide variation of estimates of propulsion system mass for an integrated spacecraft SEP design.A conservative estimate of net mass can be obtained, however, by assuming a SEP specific mass of 40-50 kg/kW, an array specific mass of 8-12 kg/kW and a propulsion tankage mass of 15% of the consumed propellant.

MAIN BELT ASTEROID RENDEZVOUS

Generally SEP spacecraft have been limited to rendezvous mission to asteroids in the inner main belt at solar distances less than around 2.5 astronomical units. Rendezvous at larger solar distances is possible however if a higher power solar array is used. Delivery capability for these missions is usually low for flight times less than two years[1] and increased performance can be achieved by allowing additional flight time. Table 1 below presents the performance for missions to several large main belt asteroids that could be launched during the first half of the next decade..

Table 1. **MAIN BELT ASTEROID RENDEZVOUS**

			Delta *7925*				Medlite Delta 7326			
	fty	tl	c3	m0	mp	mf	C3	m0	mp	mf
4 Vests V	*3.20*	11/2000	2.48	1109	357	752	2.72	556	178	377
8 Flora S	3.30	7/2001	10.37	940	226	714	9.55	471	116	355
19 Fortuna G	3.50	1/2002	3.68	1082	324	758	3.62	544	164	380
11 Parthenope S	3.25	3/2002	3.23	1092	337	754	3.35	547	170	378
9 Metis S	3.20	5/2002	3.29	1090	334	756	3.26	548	169	379
27 Euterpe S	2.90	7/2002	4.41	1065	316	749	4.34	534	159	375
5 Astraea S	3.60	6/2004	2.62	1106	362	744	2.52	558	185	374
7 Iris S	2.50	1 0/2004	6.65	1016	268	748	6.43	508	134	374
1 Ceres	3.00	5/2003	1.89	1123	309	814	1.82	568	158	410

in the above table, *fty* is the flight time in years, *tl* is the launch month and year, *c3* is the launch energy, and *m0*, *mp*, and *mf* are the initial wet spacecraft mass, propellant mass, and final dry spacecraft mass respectively. This table shows only a random sampling of possible asteroid rendezvous missions and is intended to indicate the availability of attractive targets with a final spacecraft mass in the range of 700-800 kg for a Delta class mission.

The last example shown in Table 1, that for a Ceres rendezvous mission, differs from the other asteroid rendezvous missions in that it uses a gravity assist of Mars together with a larger solar array power to achieve rendezvous with Ceres. Increasing the size of the solar array to 10 kW and 5 kW respectively for the two spacecraft options provides sufficient power to achieve rendezvous at the heliocentric distance of Ceres. Although rendezvous could be achieved with a lower array power level, increasing the power to 10 kW results in a delivery capability for Ceres that is greater than that for the asteroid targets in Table 1. A small increase in delivery capability is realized if additional thrusters are employed to use the power available at the start of the mission, however the increase in performance is not enough to justify the increased complexity of the propulsion system. Other asteroid targets at the distance of Ceres could also benefit from a Mars gravity assist when the phasing between the Earth, Mars and the asteroid are optimal.

A heliocentric plot of the spacecraft trajectory for the 10 kW Delta class Ceres rendezvous mission is shown in figure 6. Also shown in this figure are the orbits of the Earth, Mars and Ceres. Time ticks are shown along the spacecraft trajectory at 30 day intervals and coast arcs immediately prior to the Mars gravity assist are indicated by dashed lines. This same convention is also used for other trajectory plots in this paper.

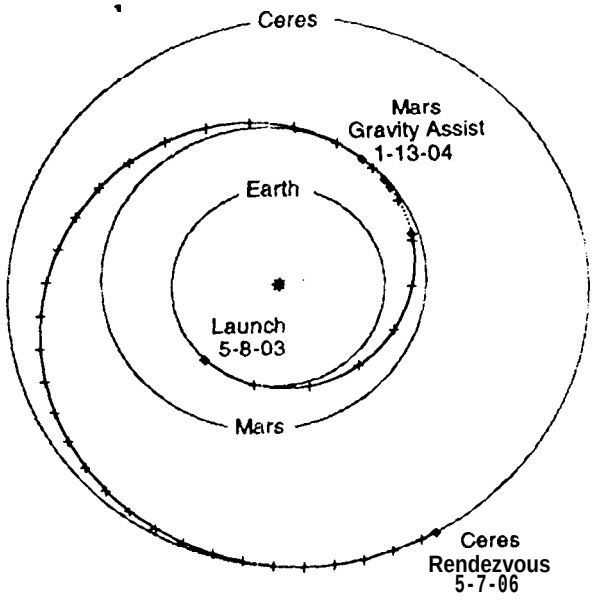

Figure 6 Ceres Rendezvous Trajectory

COMET RENDEZVOUS

Since comets generally have larger orbital energy and higher eccentricity of than the inner main belt asteroids, SEP delivery capability is not quite as good as for the asteroid missions described in the previous section. Because of the high eccentricity of comet orbits, the optimal departure point on the orbit of the Earth is usually located close to the direction of comet perihelion. The comet rendezvous trajectories described in this paper are called indirect post perihelion rendezvous and are defined as having more than one complete revolution around the sun before arriving at the comet several hundred days after comet perihelion. Rendezvous at the comet orbit generaLly occurs at a distance from the sun where the array power has dropped to that corresponding to the minimum throttle point of the thrusters. Earlier arrivals are possible closer to perihelion with some degradation of performance.

Because of the high energy and eccentricity of these comet orbits, no more than one or two launch opportunities have good performance for a particular comet apparition. Multiple launch opportunities would occur a year apart, the first occurring around three years before comet perihelion and the second occurring around two years before comet perihelion. The best launch opportunities occur around 2.5 years prior to comet perihelion and opportunities one year before or one year after this one generally result in low mission performance. Delivery capability for some of the better known short periodic comets with good performance is shown in Table 2.

Table 2 COMET RENDEZVOUS

			Delta 7925				Medlite Delta 7326			
	fty	tl	C3	m0	mp	mf	c3	m0	mp	mf
Kopff	3.16	6/2000	10.37	940	267	673	9.86	467	134	333
Wirtanen	2.32	11/2000	11.13	926	276	649	10.06	465	142	323
Wild 2	3.27	2/2001	10.34	941	258	683	9.90	466	129	337
du Toit-Hartley	2.52	3/2001	8.06	987	237	750	7.58	494	120	374
Haneda-Campos	2.85	912001	10.42	939	230	709	9.84	467	117	351
Tempel 2	2.98	6/2002	13.41	883	253	629	12.65	436	127	309
Tempel 1	2.84	5/2003	9.02	967	297	670	8.60	482	149	332
Tuttle-Giacobini-Kre	2.84	3/2004	10.95	929	241	688	10.32	462	122	340
Schwassmann-Wac	2.61	5/2004	11.08	927	280	647	10.29	462	142	320

In the above table the names of the last two comets, *Tuttle-Giacobini-Kresak* and *Schwassmann-Wachmann3,* have been truncated because of their length. These comet

rendezvous missions, like the asteroid rendezvous missions shown in Table 1, would be launched during the first part of the next decade. The flight times for these rendezvous missions cover the range from 2.3 years to a little more than 3 years. The final spacecraft mass for the more interesting cornet missions ranges from 600 to 700 kg for the Delta class missions and 300 to 35o for the Medlite class mission.

A plot of the heliocentric trajectory of the spacecraft for the 10kW Delta class mission to the short period comet Kopff is shown in Figure 7. This trajectory has a 180 day coast during the midpoint of the trajectory. Rendezvous with Kopff occurs 230 days after comet perihelion at a solar distance of 2.6 astronomical units.

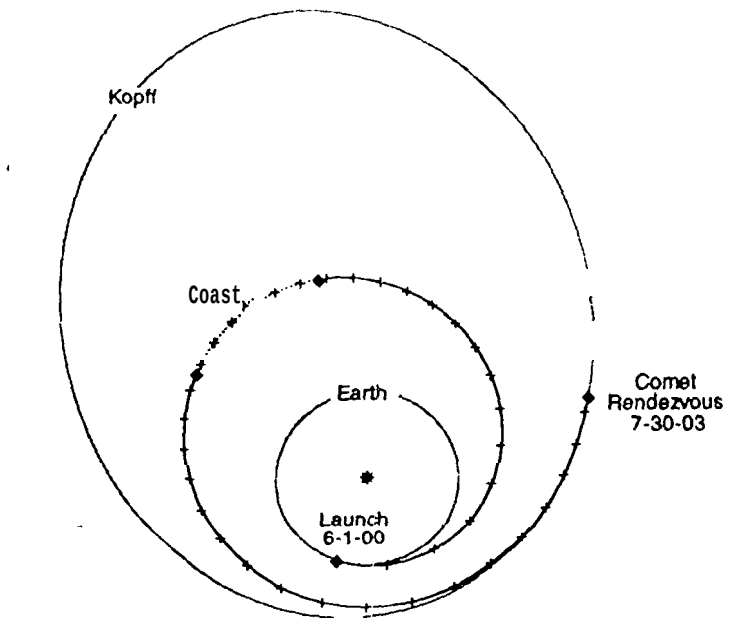

Figure 7 Kopff Rendezvous Trajectory

COMET SAMPLE RETURN

An example of an all SEP comet sample return mission is presented here for a mission to Tempel 1. The main concern with this all SEP sample return mission is that considerable thrusting at large solar distances is required to return to the Earth. In order to handle this large variation in solar array power, an increase in array power to 8 kW and a thruster throttling strategy that allowed either one or two operating thrusters was adopted. This sample return mission does not appear feasible using the smaller Medlite class spacecraft and only a mission using the larger Delta class spacecraft appears feasible. A stay time of 60 days is allowed at the comet in order to handle the initial reconnaissance and mapping of the comet followed by the sample acquisition phase. An allowance for a 50 kg science package to be left on the comet was also assumed for this mission.

The launch energy for the Kopff rendezvous mission is 6.62 km^2/s^2 and results in an initial injected spacecraft mass of 1017 kg. The propellant consumption was 357 kg and resulted in a return spacecraft mass of 610 kg. This return spacecraft mass must include an allowance for an aero-capture Earth return capsule which would enter the atmosphere at a relative speed of 14 to 15 km/s. Figure 8 is a plot of the heliocentric trajectory of this sample return mission. Note that there are two thrust phases on the Earth return leg from the comet. The first thrust phase at comet departure mainly adjusts the spacecraft to earth phasing by reducing the spacecraft heliocentric energy. The second thrust phase basically reduces the spacecraft perihelion to that of the Earth. The resulting hyperbolic excess speed of 10 km/s is the optimal value and can be reduced somewhat by increased thrusting on the inward portion of the return trajectory. Thrusting occurs to nearly a solar distance of 3.8 astronomical units where the uncertainty of the array power could have a major influence on the performance for this mission.

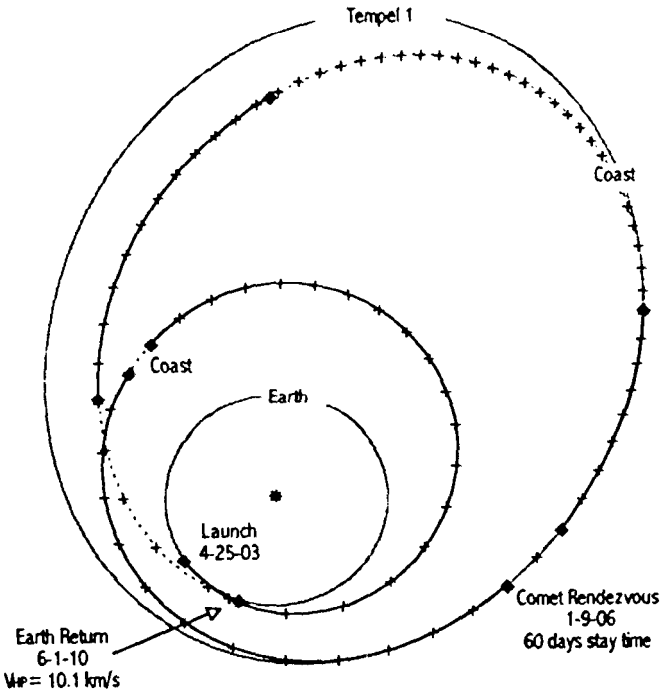

Figure 8 Tempel 1 Sample Return Mission

OUTER PLANET MISSIONS

Solar Electric Propulsion presents its greatest advantage as compared with conventional chemical propulsion spacecraft in performing rendezvous missions to asteroids and comets. There may also be advantages in using the technology for other types of missions. One class of missions that could use SEP advantageously is that of outer planet missions. In this class of missions SEP is used more like an enhanced upper stage of the launch vehicle. Since it is impractical to continue thrusting at the

distances of any of the outer planets, an additional chemical propulsion stage is necessary for the orbit insertion phase of outer planet orbiter missions. In the case of a flyby mission such as that of a flyby of Pluto, only a small chemical mono-propellant stage is required for attitude control and small navigational corrections following SEP thrust termination.

Although it is possible to fly these missions using an indirect trajectory transfer mode similar to that used for comet missions, the performance is generally marginal for Jupiter missions and low for missions further away from the sun. In this case advantage can be taken of gravity assists of the Earth or Venus. Single gravity assists of the Earth are the most advantageous because mission opportunities are not constrained by the ephemeris of three planetary bodies but of only of two, the Earth and the target. Consequently launch opportunities occur every synodic period of the Earth and target. Introducing Venus as a gravity assist body constrains the launch opportunities and further requires the spacecraft to thrust at solar distances approaching 0.7 astronomical units. Examples of the different types of outer planet transfer trajectories are shown in the next sections.

JUPITER ORBITER MISSIONS

A number of different trajectory types are presented for this mission using various combinations of Venus and Earth gravity assists. As a common denominator in comparing the different trajectory types for this mission, a freed arrival hyperbolic excess speed at Jupiter was specified. In order to keep the magnitude of the orbit insertion maneuver low, a low value of this excess speed is desirable. However it is quite difficult to get arrival excess speeds much below 6-6.5 km/s for trajectory types that have Venus as the last gravity assist body and as a consequence an excess speed of 6.5 km/s at Jupiter was used to compare the various trajectory types.

In addition to an indirect transfer trajectory with no planetary gravity assists, trajectories were considered that included single gravity assists of the Earth (EGA) or Venus (VGA), two gravity assists of Venus (VVGA) or a gravity assist of Venus followed by a gravity assist of the Earth (VEGA). The closest approach altitudes for these gravity assists were constrained to 300 km unless the optimization criteria allowed more distant flybys.

Table 3 presents a tabulation of the results of this comparison. As expected the indirect transfer trajectory yields the lowest performance with the trajectory with a single Venus gravity assist slightly better. The performance is about the same for trajectories with a single Earth gravity assist and ones with a double Venus gravity assist. The best performance is realized for the Venus-Earth gravity assist trajectory. Note that these conclusions only apply to the particular examples presented here. Other launch opportunities may make those trajectories involving a Venus gravity assist either better or worse than those shown in Table 3. In general the performance for both the indirect trajectory and single Earth gravity assist trajectory vary only slightly from one Earth-Jupiter launch opportunity to the next.

Table 3. JUPITER ORBITER TRAJECTORIES

			Delta *7925*				Medlite Delta 7326			
trajectory type	fty	tl	C3	m0	mp	mf	C3	m0	mp	mf
Indirect	4.35	11 /2002	9.17	964	221	743	8.56	482	114	368
EGA	3.43	9/2002	.91	1146	198	948	.73	583	103	480
VGA	4.60	1 2/2002	7.68	995	196	799	7.29	497	101	396
W G A	4.55	7/2002	2.84	1101	153	948	2.77	555	78	477
VEGA	5.08	4/2003	.76	1150	132	1018	.59	585	69	516

A plot of the trajectory for the Earth Gravity Assist mission in Table 3 is shown in Figure 9 below. This gravity assist trajectory trajectory differs from the more usual two year SEP Earth gravity assist trajectory shown later in this paper for a Uranus orbiter mission in using a shorter one and a quarter year Earth return. This shorter Earth return trajectory shows superior performance for low energy outer planet trajectories such as that for a Jupiter orbiter mission than the performance for the more usual two year Earth return gravity assist. An additional benefit of this transfer trajectory is a one year shorter transfer time than that for the other trajectory types considered in table 3. A possible disadvantage of this trajectory is that the spacecraft must thrust inside the orbit of the Earth.

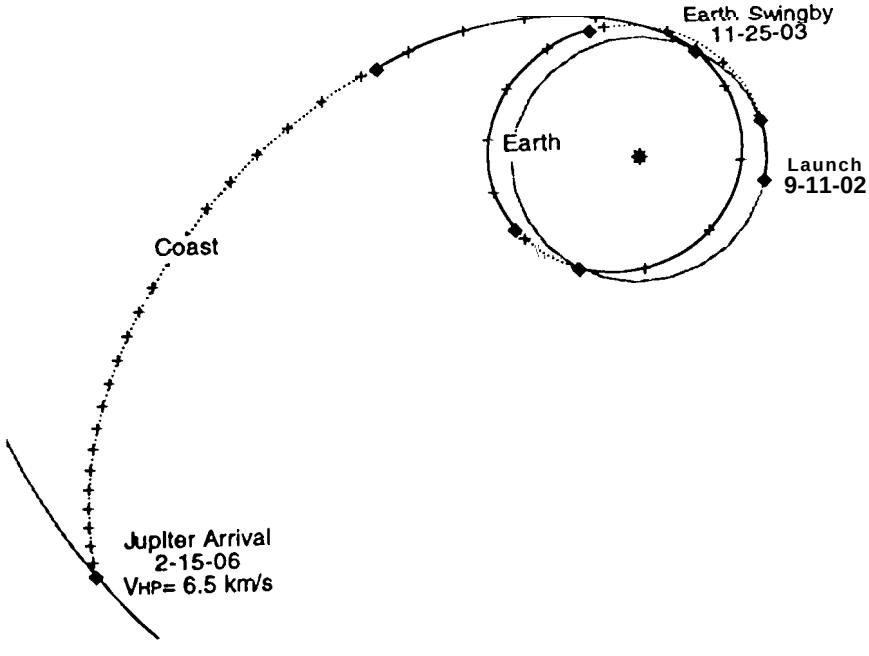

Figure 9 SEP Earth Gravity Assist Jupiter Orbiter Trajectory

URANUS ORBITER AND PLUTO FLYBY MISSIONS

The trajectories for these two missions represent some of the more complex SEP trajectories. 'A performance summary is presented for these two missions in Table 4 below for the two launch vehicle/SEP combinations.

Table 4 URANUS ORBITER AND PLUTO FLYBY

			Delta 7925				Medlite Delta 7326			
	fty	tl	c3	m0	mp	mf	C3	m0	mp	mf
Uranus EJGA	14.00	11/2004	8.78	972	128	844	8.24	486	68	418
Pluto WJGA	10.20	7/2002	4.81	1056	210	846	4.62	530	107	423

The trajectory for the Uranus mission uses a two year Earth gravity assist followed by a gravity assist of Jupiter. Since this mission is an orbiter, a low arrival excess speed was desired and required a total flight time of 14 years. The propulsion requirements for this mission were relatively modest, there being only two thrust arcs in the trajectory, the first occurring immediately after launch and the second of around 200 days duration occurring at aphelion prior to the Earth gravity assist. The remainder of the trajectory including all that following the Earth gravity assist is ballistic. A plot of the first portion of this trajectory prior to the Jupiter gravity assist is shown in Figure 10. Indicated in this figure are the directions of the flyby of Jupiter and the arrival at Uranus.

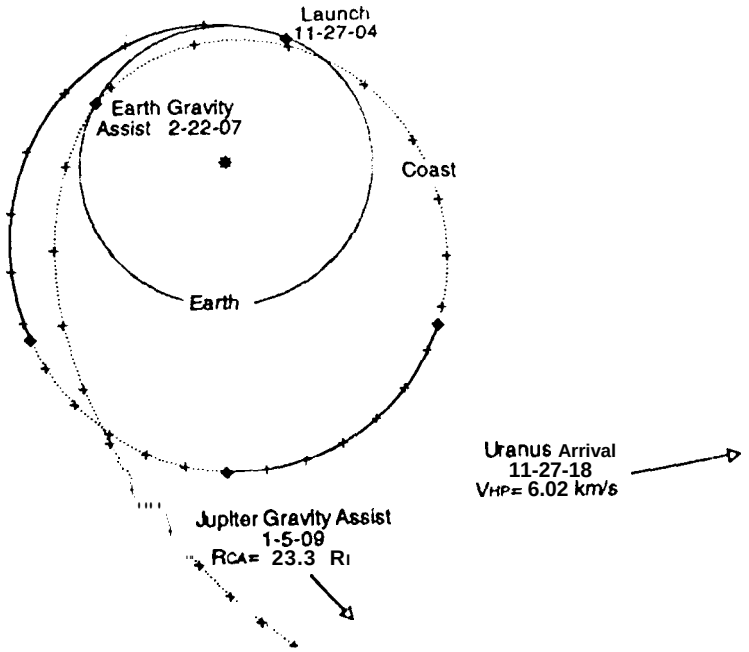

Figure 10 Earth-Jupiter Gravity Assist Uranus Orbiter trajectory

The Pluto flyby trajectory employs a two flybys of Venus followed by a flyby of Jupiter to achieve the necessary energy for 10 year mission to Pluto. In order to achieve this short flight time to Pluto, a relatively fast flyby of Jupiter at a hyperbolic excess speed of 1[5].4 km/s is required with a resulting closest approach to Jupiter of 5.6 Jupiter radii. This high energy flyby of Jupiter requires a substantial amount of thrusting around both Venus flybys. The relative phasing of the Earth, Venus, Jupiter and Pluto is very favorable for this particular launch opportunity and later launch opportunities in succeeding years display considerably lower performance. A plot of the first portion of this trajectory prior to the Jupiter gravity assist is shown in Figure 11. Indicated in this figure are the directions of the flybys of Jupiter and Pluto.

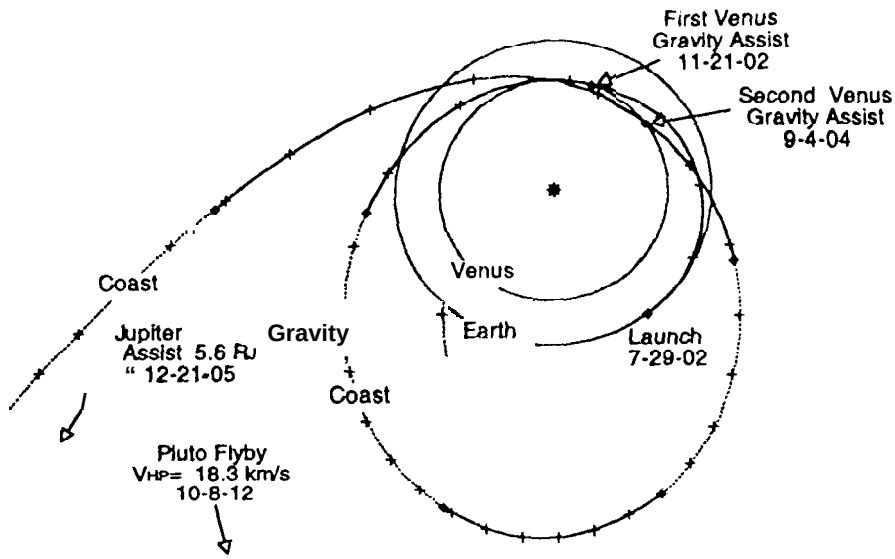

Figure 11 Venus-Venus-Jupiter Gravity Assist Pluto Flyby

VENUS GRAVITY ASSIST MERCURY ORBITER

There has been much interest in the past several years in ballistic missions to Mercury using one or more gravity assists at Venus to provide acceptable payloads[5]. Several investigators have also examined this type of Venus gravity assist Mercury mission using a Solar Electric Propulsion Spacecraft[6,7]. Past studies of a SEP Mercury rendezvous mission without a Venus gravity assist usually employed a higher thrust acceleration and resulted in a transfer time of two years or less and lower performance than that achievable by including a Venus gravity assist in the trajectory..

The example of the Mercury orbiter mission presented in this paper employs a reference array power level of 3 kW and 1.5 kW respectively for the Delta and Medlite class missions. The solar array differs from that used for the planetary missions described previously in that it is not *only* smaller, but also assumes the use a Ga/As/Ge

solar array which appears more suitable for this type of mission with significant thrusting at close solar distances. Because the power available to the thrusters at the start of the trajectory is less than the maximum thruster power, the thrusters are throttled initially until the spacecraft passes inside the orbit of Venus. At this point sufficient power is thereafter available to operate the thrusters at full power.

In the exampe used in this paper the spacecraft would be launched in August 2002 and arrive in December 2004 after a flight time of 848 days. A Venus gravity assist in February 2003 is used to decrease the perihelion distance of the transfer trajectory to nearly that of Mercury. The spacecraft then thrusts mostly around perihelion in order to decrease spacecraft aphelion distance to that of Mercury. Table 5 below presents the performance for this mission for the two classes of launch vehicles.

Table 5. MERCURY ORBITER

			Delta 7925				Medlite Delta 7326			
	fty	tl	c3	m0	mp	mf	c3	m0	mp	mf
Mercury	2.32	8-27-02	5.44	1042	287	755	5.35	521	144	377

Note that the above performance only represents arriving at Mercury with zero hyperbolic excess speed. No attempt has been made to calculate performance for achieving any particular orbit around Mercury including spiral capture using the SEP. A plot of the trajectory for this Mercury orbiter mission is shown in Figure 12 which clearly indicates the numerous coast periods.

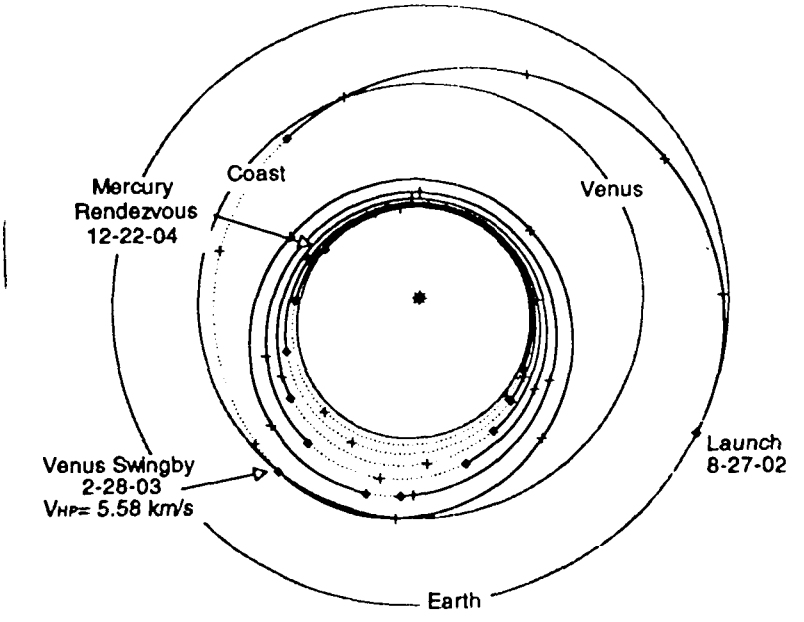

Figure 12 Mercury Orbiter Trajectory

The presence of coast arcs around spacecraft aphelion indicate that thrusting at this time is not effective. Thrusting following the Venus flyby must primarily reduce spacecraft aphelion with only a slight reduction in perihelion required. Thus thrusting is most effective around perihelion and if coast arcs are present, they will naturally appear around aphelion. This trajectory performs 6.5 revolutions around the sun before arriving at Mercury and coast phases appear around aphelion on each pass around the sun with the coast arc getting longer with each succeeding orbit. Slight changes in the power or propulsion system parameters can have a major effect on the location of the arrival point on the orbit of Mercury and can result in a greater or fewer number of orbits around the sun.

SUMMARY AND ACKNOWLEDGMENTS

This paper has presented an overall survey of performance for a representative set of planetary missions that may be most amendable to the use Solar Electric Propulsion. The mission performance presented here is based upon current estimates of performance for the 2.5 KW 30cm NSTAR Xenon engines. Advancements in thruster technology including developments of smaller, lower power thrusters will likely not change the delivery capability presented in this paper to any great extent. Most of these advancements will address both thruster operating lifetime and thrust subsystem mass and would have an impact on the actual delivered payload rather than on total delivered spacecraft mass.

The various SEP spacecraft trajectories presented in this paper were calculated to support numerous mission studies at the Jet Propulsion Laboratory that considered SEP as one of the propulsion options to be considered. The author wishes to thank the numerous individuals in the above studies for their support. Also the author would like to acknowledge the assistance of John Brophy of JPL and other individuals at the NASA Lewis Research Center for the data on thruster performance, and the support of Roy Kakuda and the NSTAR project office for the overall mission studies.

References

1. Sauer, Carl G., Jr, *Planetary Mission Performance for Small Solar Electric Propulsion Spacecraft,* Paper AAS 93-561, AAS/AIAA Astrodynamics Specialist Conference, Victoria, BC, Canada, Aug 16-19, 1993

2. Sauer, Carl G., Jr, and Yen, Chen-Wan, *Planetary Mission Capability of Small Low Power Solar Electric Propulsion Systems,* Paper L4A-L-0706, IAA International Conference on Low-Cost Planetary Missions, Laurel, Md, Apr 12-15, 1994

3. Rawlin, V. K., *Power Throttling the NSTAR Thruster,* AIAA Paper 95-2515, 31st AIAA/ASME/SAE/ASEE Jount Propulsion Conference and Exhibit, San Diego, CA, July 10-12, 1995

4. Polk, J. E., Anderson, J. R., Brophy, J. R., Rawlin, V. K., Patterson, M.J., and Sovey, J. S., *The Effect* of *Engine Wear on Performance in the NSTAR 8000 Hour Ion Engine Endurance Test*, Paper AIAA 97-3387, 33rd AIAA/ASME/SAE/ASEE Joint Propulsion Conference and Exhibit, Seattle, WA., July 6-9, 1997

5. Yen, C. W., *Ballistic Mercury Orbiter Mission via Venus and Mercury Gravity Assists, Paper AAS 85-346,* AAS/AIAA Astrodynamic Conference, Vail, CO, Aug **12-15, 1985.**

6. Kluever, Craig.A., and Abu-Saymeh, Mudar, *Mercury Mission Design Using Solar Electric Propulsion Spacecraft,* Paper AAS 97-173, AAS/AIAA Space Flight Mechanics Meeting, Huntville, AL, Feb **10-12, 1997.**

7. Yamakawa, H., Kawaguchi, J., Uesugi, K., and Matsuo, H., *Frequent Access to Mercury* in the *Early* 2s' *Century: Multiple Mercury Flyby Mission via Electric Propulsion,* Acts Astronautica, Vol. 39, No. **1-4,** pp 133-142, 1996.